

A. Al-Rabiah¹A. Ajbar¹

¹ Department of Chemical Engineering, King Saud University, Riyadh, Saudi Arabia

Research Article

Study of the Operability of a Continuous Bioreactor for the Pre-fermentation of Cheese Culture

The dynamics of a continuous stirred-tank bioreactor for cheese pre-fermentation is analyzed using elementary concepts of bifurcation theory and continuation techniques. The bioreactor model, which was previously developed and validated, explicitly incorporates the effect of uncontrolled pH levels. The stability analysis of the model is carried out for two cases: In the first case, the bioreactor is equipped with a seed tank, while the second case involves no additional seed tank. The static analysis allows useful analytical results for the study of steady state multiplicity of the model to be derived. The results of this paper provide practical guidelines on the selection of operating parameters that can eliminate difficult operating regions and that can consequently improve the operability of the bioreactor.

Keywords: Bioreactors, Food processing, Modeling, Reactors – Continuous stirred tank

Received: April 25, 2007; *revised:* August 16, 2007; *accepted:* September 4, 2007

DOI: 10.1002/elsc.200720215

1 Introduction

Bioreactor control has become an active area of research in recent years [1–5]. This is partially attributable to the difficulty in controlling the highly non-linear behavior associated with such systems. Bioreactors are generally full of operational problems that manifest themselves essentially in the form of input and output multiplicities [6]. Input multiplicities arise when different values of a manipulated input variable produce the same value of the controlled output variable. When input multiplicities occur, there is always the possibility of a transition from one steady state to another without detecting it. Moreover, input multiplicity implies the existence of regions where the zero dynamics are unstable (the corresponding linearized system has right-half plane zeros). The presence of such behavior is known to limit the closed loop performance, regardless of the selected control algorithms. Output multiplicities are also known to occur in bioreactors. This type of multiplicity arises when for the same value of an input variable, different responses to the chosen controlled output are obtained. It is well known that the presence of an S or inverse S shaped input-output is associated with the hysteresis phenom-

enon, which results in a region of open loop unstable behavior. Output multiplicities are also known to have an adverse effect on control performance. The detection of these multiplicities in the bioreactor is an important task. This task requires two elements: a good model of the process and adequate tools for the analysis. There are a number of theoretical tools that can guide the static and dynamic analysis of bioreactors. Among them the singularity theory has been proven to be an adequate tool for this task. The theory, which was successfully applied to chemical reactors [7–12], provides a useful framework for classifying branching phenomena in which different types of multiplicity of the nonlinear model can be classified. In this regard a useful picture of the different behavior can be constructed in the parameter space of the model. This allows the delineation of regions of unsafe/unstable behavior to be predicted by the model.

This paper addresses the issue of bioreactor operability when applied to a continuous pre-fermentation of cheese culture. Cheese manufacture is traditionally a batch process, but with an ever increasing cheese consumption, a mass production of cheese is of great interest to the dairy industry. For this reason, the study of a potential continuous process for cheese manufacture would be a step in the right direction to achieve two goals: The first is to study the improvement in the bioreactor productivity, while the second objective is to analyze the potential operating problems that may be inherent in the continuous bioprocess. A number of models have been developed in the literature for cell growth and lactic acid production [13–17]. However, these models were limited to either con-

Correspondence: A. Ajbar (aajbar@ksu.edu.sa), Department of Chemical Engineering, King Saud University, P.O. Box 800, Riyadh 11421, Saudi Arabia

stant or optimally controlled pH values. These models may present some shortcomings since the cheese pre-fermentation process is known to be a hydrogen ion dependent process, as the pH of milk changes with cell growth and lactic acid production. Recently, Funahashi et al. [18] proposed a kinetic model that can predict growth and lactic acid production in pre-fermentation without external pH control. The proposed model was shown to simulate well uncontrolled pH experiments. Lee and Lim [19] carried out a local stability analysis for the model. The authors showed that for given values of kinetic parameters the model can predict steady state multiplicity. The authors also studied the case where a seed tank was added to the bioreactor. Their analysis showed that the addition of the seed tank provides a stabilizing effect on the bioreactor dynamics.

The objective of this paper is to study the operability of the same bioreactor model. This analysis shows that analytical results can be obtained that determine the exact type of multiplicity that may be predicted by the model. Steady state uniqueness, saddle-node, hysteresis as well as pitchfork singularities are shown to occur in the bioreactor model. The effect of operating parameters on the occurrence/removal of these singularities is analyzed. It is also shown how practical diagrams in terms of operating parameters of the model can be constructed that delineate the different multiplicity regions. The organization of the paper starts with the description of the process model, followed by the analysis of static behavior. The general model for the bioreactor with the additional seed tank is first studied, followed by the analysis of the bioreactor alone. A final note is to be made about the approach used in the analysis. The singularity theory has been successfully used since the early eighties [6–12, 20] for the study of the stability behavior of lumped parameter reactive systems. Recently, the author of this paper has used the theory to revisit the stability behavior of a number of unstructured kinetic models of continuous bioreactors [21–23]. The paper is self-contained but the reader may consult the reference book [24] for more details about the theory.

The novelty of this paper is that it addresses the issue of operability of bioreactors. While the operability of chemical reactors has been extensively studied in the literature [7–12], this is not the case for bioreactors. This paper illustrates how modeling decisions (and ultimately the design and the operating parameters) influence the operating characteristics of the bioreactor.

2 Process Model

The unsteady state mass balances for the different species in the bioreactor shown in Fig. 1 are described by the following ordinary differential equations,

$$\frac{dX}{dt} = \frac{F_2 X_f - F_3 X}{V} + \mu X \quad (1)$$

$$\frac{dS}{dt} = \frac{F_1 S_f - F_3 S}{V} - \sigma X \quad (2)$$

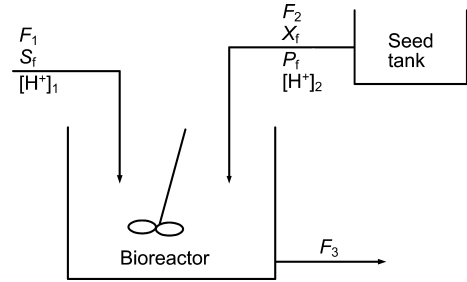


Figure 1. Schematic diagram of the bioreactor-seed tank system.

$$\frac{dP}{dt} = \frac{F_2 P_f - F_3 P}{V} + \pi X \quad (3)$$

$$\frac{d[H^+]}{dt} = \frac{F_1 [H^+]_1 + F_2 [H^+]_2 - F_3 [H^+]}{V} + \nu X \quad (4)$$

$$\frac{dV}{dt} = F_1 + F_2 - F_3 \quad (5)$$

X , S and P are the concentrations of cells, lactose and lactic acid, respectively, while X_f , S_f and P_f are the associated feed concentrations. $[H^+]$, $[H^+]_1$ and $[H^+]_2$ are hydrogen ion concentrations in the bioreactor, in the feed and in the seed tank, respectively. V is the volume of the bioreactor, and F_1 , F_2 and F_3 are the lactose, the seed and the exit feed rates, respectively. The different rates in the model equations have the following definitions: μ is the specific growth rate of cells, σ is the lactose consumption rate, π is the lactic acid production rate and ν is the hydrogen ion production rate. These kinetic rates have the following form:

$$\mu = \frac{\mu_0 [H^+]}{K_1 + [H^+] + [H^+]^2 / K_2} \quad (6)$$

$$\sigma = \frac{\sigma_0 [H^+]}{K_3 + [H^+] + [H^+]^2 / K_4} \quad (7)$$

$$\pi = \frac{\pi_0 [H^+]}{K_5 + [H^+] + [H^+]^2 / K_6} \quad (8)$$

$$\nu = \frac{\nu_0 [H^+]}{K_5 + [H^+] + [H^+]^2 / K_6} \quad (9)$$

The model rational and assumptions were given in [18–19]. A note should, however, be made about some peculiarities of the model. The specific kinetic rates (Eqs. (6–9)) are assumed to depend solely on the hydrogen ion concentration. The authors showed that this assumption is adequate only when the system involves high lactose and low lactic acid concentrations. An appropriate experimental validation was also carried out by the authors [18]. The steady state model is obtained by setting the left hand sides of Eqs. (1–5) to zero. Introducing the bioreactor dilution rate D defined by $D = F_3/V$, the ratio of seed to substrate feed rate, $a = F_2/F_1$, and using the fact that $F_3 = F_1 + F_2$, the steady state model can be written as follows:

$$D\left(\frac{aX_f}{1+a} - X\right) + \mu([H^+])X = 0 \quad (10)$$

$$D\left(\frac{S_f}{1+a} - S\right) - \sigma([H^+])X = 0 \quad (11)$$

$$D\left(\frac{aP_f}{1+a} - P\right) + \pi([H^+])X = 0 \quad (12)$$

$$D\left(\frac{[H^+]_1}{1+a} + \frac{a[H^+]_2}{1+a} - [H^+]\right) + v([H^+])X = 0 \quad (13)$$

Following the assumption that the specific kinetic rates are $[H^+]$ dependent only, it can be noted that the mass balance equations for cells and $[H^+]$ concentrations (Eqs. (10) and (13)) do not include lactose or lactic acid concentrations. Therefore, these two equations can be considered as a system of two independent variables. Eq. (10), in particular, would yield,

$$X = \frac{aDX_f}{(1+a)(D - \mu([H^+]))} \quad (14)$$

Substituting in Eq. (13) yields the following algebraic equation for $[H^+]$

$$\frac{[H^+]_1}{1+a} + \frac{a[H^+]_2}{1+a} - [H^+] + \frac{aX_f}{(1+a)} \frac{v([H^+])}{(D - \mu([H^+]))} = 0 \quad (15)$$

Substituting for X (Eq. (14)) in Eqs. (11)–(12) yields the expressions for S and P , respectively

$$S = \frac{S_f}{1+a} - \frac{\sigma([H^+])X}{D} \quad (16)$$

$$P = \frac{aP_f}{1+a} + \frac{\pi([H^+])X}{D} \quad (17)$$

3 Study of the Model Multiplicity

The nonlinear model (Eqs. (10–13)) can exhibit a number of steady state multiplicities that can influence the control of the process. The study of these multiplicities and the associated process control ramifications can be suitably carried out within the framework of the singularity theory. The starting point of the analysis is to see whether the steady state equations of the model can be reduced to a single variable algebraic equation. This is fortunately the case in the studied model. Looking at Eq. (15) it can be seen that the model equation has collapsed into this single algebraic equation. Eq. (15) is written in the following compact form:

$$F([H^+], u) = 0 \quad (18)$$

where $[H^+]$ is the output (controlled variable) and u is the selected input or manipulated variable, which is a distinguished parameter in the singularity theory. Excluding the assumed constant kinetic parameters, it can be seen that the single algebraic equation (Eq. (15)) includes a number of potentially variable operating parameters. These include the dilution rate

D , the ratio a of seed to substrate feed rates, the feed pHs ($[H^+]_1$ and $[H^+]_2$) and the cells feed concentration X_f . The two other operating parameters S_f and P_f that exist in the original model are not present in this equation (Eq. (15)). This is due, as mentioned earlier, to the decoupling between Eqs. (10–13), on the one hand and Eqs. (11–12), on the other. Consequently for this model, these two parameters will not have an effect on the model multiplicity. However, they will have an effect on setting boundaries for the meaningful existence of steady state solutions of the model, since the following natural constraints: $X > 0$ and $0 < S < S_f$ should always be satisfied.

In the following section it is examined which of the mentioned parameters, if chosen as the manipulated variable, can lead to multiplicity in the nonlinear model. From a control point of view, both input and output multiplicities should be considered. The necessary conditions for the existence of input multiplicity for the variable u are that

$$F = \frac{\partial F}{\partial u} = 0 \quad (19)$$

while the necessary conditions for output multiplicity are that

$$F = \frac{\partial F}{\partial [H^+]} = 0 \quad (20)$$

Input or output multiplicities, when they occur, manifest themselves in the form of a specific behavior, as the selected manipulated variable is varied. These types of behavior are called static singularities. Fig. 2 shows how the basic singularities can predict a nonlinear model. The simplest static bifurcation is the saddle-node bifurcation (see Fig. 2A). It can be seen from the figure that saddle-node bifurcation is one form of output multiplicity. The diagram arises by joining two branches of the curves of the solution: one branch consists of locally stable solutions while the other branch consists of lo-

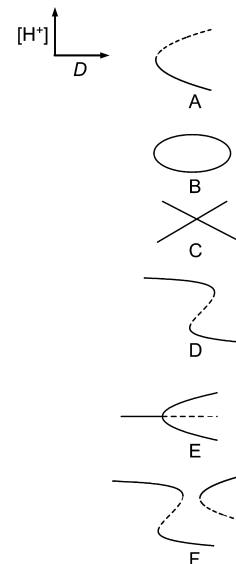


Figure 2. Various static singularities: (A) saddle-node; (B) isola; (C) mushroom; (D) hysteresis; (E) pitchfork; (F) singularity that may result from perturbations of the pitchfork.

cally unstable ones. The necessary conditions for the existence of this singularity are given in Eq. (20) in addition to:

$$\frac{\partial F}{\partial [u]} \neq 0 \quad \text{and} \quad \frac{\partial^2 F}{\partial [H^+]^2} \neq 0 \quad (21)$$

The first condition implies that a unique curve of steady state solutions passes through the bifurcation point, while the second equation implies that the curve lies on one side of the steady state solutions. Should either one or both the above conditions be violated, then this will give rise to higher order singularities. The second possible change that can occur in the steady state locus is the formation of an isola and the development of isola into a mushroom, as shown in Figs. 2B–C. These singularities can involve both input and output multiplicities. They arise when the following conditions are satisfied

$$F = F_{[H^+]} = F_u = 0 \quad (22)$$

and

$$F_{[H^+]u} \neq 0, F_{[H^+][H^+]} \neq 0, F_{uu} \neq 0 \quad (23)$$

F_x and F_{xx} designate the first and second order partial derivatives of F with respect to (x) , respectively. The third qualitative change in the behavior of the model is the appearance of S or an inverse S-shaped behavior as shown in Fig. 2D. This is the famous hysteresis singularity that produces output multiplicity. For chemical reactors, the S-shaped input-output curve is associated with ignition/extinction behavior. For bioreactors it is generally associated with a jump from low to high operating conditions such as low and high substrate conversion. The last singularity to be considered is the pitchfork singularity (see Fig. 2E). The bifurcation diagram shows two curves of equilibrium intersected at the singularity. Pitchfork singularity is an example of both input and output multiplicities. This can be seen in Fig. 2F showing an example of diagrams that can arise when slight perturbations of parameters are made around the basic pitchfork diagram of Fig. 2E. The conditions of the existence of pitchfork are

$$F = F_{[H^+]} = F_u = F_{[H^+][H^+]} = 0 \quad (24)$$

and

$$F_{[H^+]u} \neq 0 \quad \text{and} \quad F_{[H^+][H^+][H^+]} \neq 0 \quad (25)$$

By characterizing the type of static singularity which the model can predict, one can understand how to minimize or even eliminate the associated multiplicity. In particular if the multiplicity between $[H^+]$ and any of the operating parameters is eliminated then the bioreactor will be generally easier to control and safer to operate, since the process gain would remain with the same sign over the operating region of interest. However, this does not guarantee that the bioreactor is asymptotically stable, since limit cycles (periodic behavior) can also occur. But in this study the focus is only on the analysis of static behavior. Now the attention of the authors should be turned to examine the conditions for input and output multiplicity in

the model. In a later section, the different singularities are studied.

The derivatives of F (Eq. (15)) with respect to $[H^+]_1$, $[H^+]_2$, $X_f D$ and a , respectively, yield:

$$\frac{\partial F}{\partial [H^+]_1} = \frac{1}{1+a} \quad (26)$$

$$\frac{\partial F}{\partial [H^+]_2} = \frac{a}{1+a} \quad (27)$$

$$\frac{\partial F}{\partial X_f} = \frac{a}{(1+a)} \frac{v}{(D-\mu)} \quad (28)$$

$$\frac{\partial F}{\partial D} = -\frac{aX_f}{(1+a)} \frac{v}{(D-\mu)^2} \quad (29)$$

$$\frac{\partial F}{\partial a} = -\frac{[H^+]_1}{(1+a)^2} + \frac{[H^+]_2}{(1+a)^2} + \frac{X_f v}{(D-\mu)(1+a)^2} \quad (30)$$

A number of conclusions can be reached from these equations. First, since $\partial F / \partial [H^+]_1$ (Eq. (26)) is always non nil then the model can never predict input multiplicity with respect to the feed pH ($[H^+]_1$). From Eqs. (27–28) it is evident that the existence of input multiplicity with respect to $[H^+]_2$ or X_f is only possible when $a = 0$ (i.e. the case where no seed tank is present). This particular case will be treated in a later section. From Eq. (29) it can also be seen that input multiplicity with respect to the dilution rate can only occur when $a = 0$ or $X_f = 0$. Again these special cases are treated independently in a later section.

The derivative of F with respect to a (Eq. (30)) provides, on the other hand, explicit conditions for the possible existence of input multiplicity. It can be therefore concluded that for the general case of $a \neq 0$ and $X_f \neq 0$ the model can predict input multiplicity only when a is varied. Moreover it could be concluded that with the absence of input multiplicity for $[H^+]_1$, $[H^+]_2$ and D , it is also anticipated that isola-mushroom (see Figs. 2B and C) and pitchfork (see Fig. 2E) singularities can not occur with any of these parameters, and can occur only when a is allowed to vary. Therefore it is evident that a is an important variable which warrants some type of control action such as a feed-forward ratio control. Moreover it can be seen that the derivatives with respect to other parameters (Eqs. (26–29)) remain the same sign which is a useful piece of information when designing feed-forward controllers.

In the following, the occurrence of these singularities for a (i.e. $u = a$) is examined in more detail. The existence of an isola-mushroom singularity is conditioned by Eqs. (22–23). However it can be noted from Eq. (30) that if F_a is zero then F_{aa} will also vanish, which violates the condition of

Eq. 23. Therefore it could be concluded that an isola-mushroom singularity cannot occur for a . The conditions for the occurrence of a pitchfork in a are given by Eqs. (24–25). The condition $F_a = 0$ leads from Eq. (30) to

$$-[H^+]_1 + [H^+]_2 + \frac{X_f v ([H^+])}{D - \mu ([H^+])} = 0 \quad (31)$$

Combining this condition with that of $F = 0$ (Eq. (15)) leads to the simple condition

$$[H^+] = [H^+]_1 \quad (32)$$

Therefore the pitchfork conditions are equivalent to the following algebraic equations, evaluated at $[H^+] = [H^+]_1$

$$F_a = 0, F_{[H^+]} = 0, F_{[H^+][H^+]} = 0 \quad (33)$$

This leads to the following system of algebraic equations, again evaluated at $[H^+] = [H^+]_1$

$$-[H^+]_1 + [H^+]_2 + \frac{vX_f}{D - \mu} = 0 \quad (34)$$

$$-1 + \frac{aX_f}{(1 + a)} \frac{d\left(\frac{v}{D - \mu}\right)}{d[H^+]} = 0 \quad (35)$$

$$\frac{d^2\left(\frac{v}{D - \mu}\right)}{d[H^+]^2} = 0 \quad (36)$$

This system can be solved for given values of model parameters to construct practical diagrams that delineate the domains where a pitchfork can or cannot occur. But first, an example of pitchfork behavior is illustrated, which was obtained using the values of model parameters shown in Tab. 1 with $X_f = 1.41$ g/L, $pH_1 = 6.33$, $pH_2 = 8.49$ and $D = 0.5$ h⁻¹.

The continuity diagram obtained with the software AUTO [25] is presented in Fig. 3. It can be seen that for values of a

Table 1. Nominal values of model parameters used in the simulations, unless specified otherwise in the text.

Value	Parameter
4×10^{-7}	K_1 [g/L]
6.85×10^{-6}	K_2 [g/L]
4.88×10^{-8}	K_3 [g/L]
4.2×10^{-6}	K_4 [g/L]
1.5×10^{-6}	K_5 [g/L]
3.91×10^{-6}	K_6 [g/L]
0.51	μ_0 [h ⁻¹]
3.35×10^{-7}	ν_0 [h ⁻¹]
3.35	π_0 [h ⁻¹]
1.02	σ_0 [g/L]
80	S_f [g/L]
5.5	X_f [g/L]
5.9	P_f [g/L]
6.7	pH_1
5.5	pH_2
0.35	D [h ⁻¹]
0.03	a

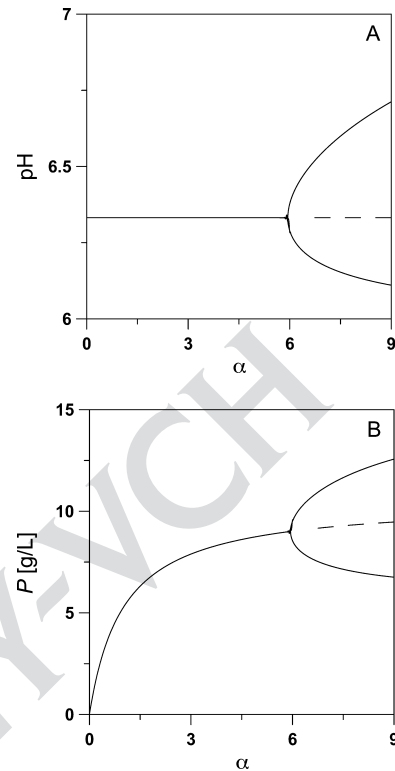


Figure 3. Continuity diagram showing pitchfork singularity in parameter spaces: (A) (a , pH) ; (B) (a , P). (Solid line, stable branch; dashed line, unstable branch).

smaller than 5.95 a single stable branch is possible, while for larger values, the system is characterized by three branches. It should be noted that the value of occurrence of multiplicity $a = 5.95$ is physically unrealistic, since the practical values of a are generally chosen smaller than unity. But with the possible variations in the kinetic parameters of the model, it is not impossible that the qualitative behavior of Fig. 3 can occur within physically realistic values of a . However in this paper the investigations are limited to the effect of the bioreactor operating parameters. Next the effect of these parameters on the boundaries of the pitchfork is studied. Fig. 4A shows the effect of a slight increase in the pH of the feed from 6.33 to 6.4. First, it can be seen that the structure of the basic pitchfork has completely changed. This is expected, since as shown in Fig. 2F, perturbations around the basic pitchfork (see Fig. 2E) in some cases can lead to other multiplicity behavior. Comparatively to Fig. 3A, where the multiplicity is born at $a = 5.95$ it can be seen in Fig. 4A that an increase in the pH of the feed also rises the range to around $a = 12$. Therefore an increase in the feed pH has a stabilizing effect on the bioreactor. Fig. 4B shows, on the other hand, the effect of a decrease in the pH of the seed tank. Again, the pitchfork singularity has changed, and the range of multiplicity is pushed to larger values of a . A decrease in the pH of the seed tank stabilizes the behavior of the bioreactor. Fig. 5A shows the effect of an increase in the cell concentration of the feed, from 1.41 to 1.45 (g/L). It is evident that the increase in X_f also stabilizes the bioreactor. Finally, Fig. 5B

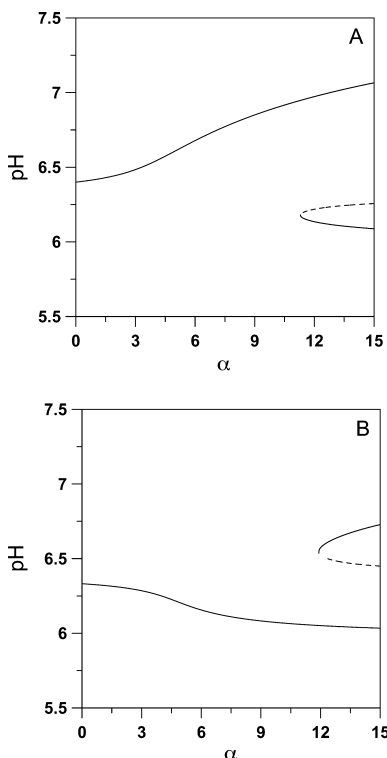


Figure 4. Continuity diagrams showing the effect on the pitchfork of Fig.3: (A) an increase in pH of feed; (B) a decrease of pH from seed tank. (Solid line, stable branch; dashed line, unstable branch).

demonstrates the effect of a decrease in the dilution rate, from 0.50 to 0.49 h⁻¹. It can be seen that a decrease in D has also a stabilizing effect on the bioreactor, since the range in terms of a of the stable steady state uniqueness is increased.

Having examined the input multiplicities, the attention is turned to the study of possible output multiplicities. The existence of the hysteresis singularity is defined by the conditions of Eqs. (24–25). Taking the derivatives $F_{[H^+]}$, $F_{[H^+][H^+]}$ yields the following conditions for hysteresis, along with the condition $F = 0$,

$$-1 + \frac{aX_f}{(1+a)} \frac{d\left(\frac{v}{D-\mu}\right)}{d[H^+]} = 0 \quad (37)$$

$$\frac{d^2\left(\frac{v}{D-\mu}\right)}{d[H^+]^2} = 0 \quad (38)$$

Together with these equations, the other non-nil derivatives (Eqs. (25)) must be satisfied. Using the expression of $F_{[H^+]}$ (Eq. (37)), it can be seen that it does not involve $[H^+]_1$ or $[H^+]_2$. Therefore $F_{[H^+][H^+]_1} = F_{[H^+][H^+]_2} = 0$ and the hysteresis cannot exist if either $[H^+]_1$ or $[H^+]_2$ are varied. For X_f it is evident that $F_{[H^+]X_f}$ is non nil except for the particular case of $a = 0$. When, on the other hand, a or D are chosen as input variables then the conditions $F_{a[H^+]}$ and $F_{D[H^+]}$ can be shown to be non nil except when X_f or $a = 0$. Therefore it could be concluded that the model can predict hysteresis only when a or D are varied. Fig. 6 presents an example of hysteresis behavior

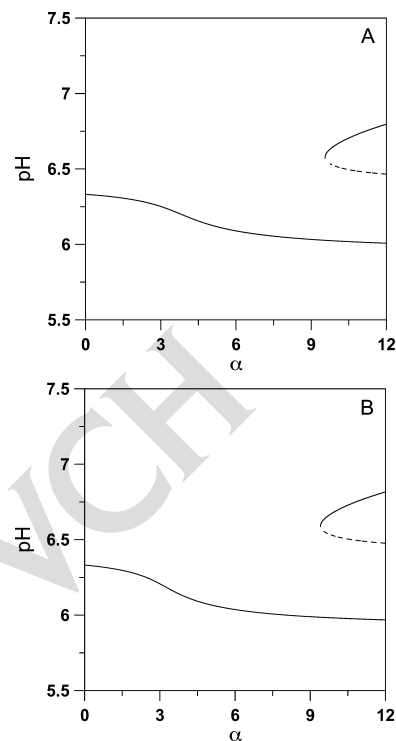


Figure 5. Continuity diagrams showing the effect on the pitchfork: (A) an increase in cell concentration of the feed X_f ; (B) a decrease in dilution rate D . (Solid line, stable branch; dashed line, unstable branch).

as a function of a , for values given in Tab. 1. The multiplicity in the hysteresis loop extends from physically realistic values of a from 0.011 to 0.037, which correspond to the limit points LP₁ and LP₂. The hysteresis boundaries are, on the other hand, shown in Figs. 7A–C. In each figure there are two curves that cross at a certain point. These curves correspond to the locus of each limit point. Hysteresis behavior is therefore confined between the two curves. Fig. 7A shows that the hysteresis exists only for pH₁ values larger than 6.05. Moreover, as

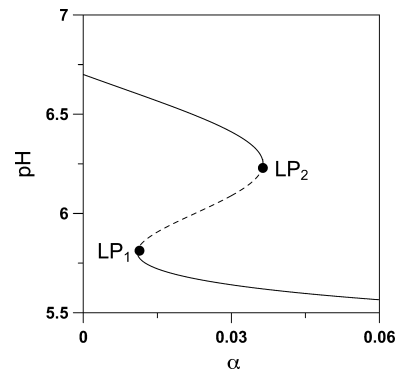


Figure 6. Continuity diagrams showing the hysteresis in a . (solid line, stable branch; dashed line, unstable branch; LP₁, LP₂ are static limit points).

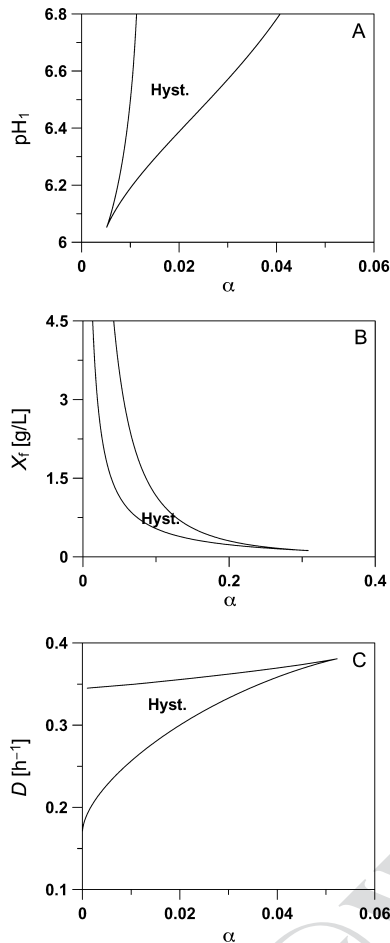


Figure 7. Diagram showing the domain of the hysteresis in the parameter spaces: (A) (pH_1, α) , (B) (X_f, α) , (C) (D, α) .

the values of pH_1 increase, the hysteresis domain (in terms of α) also increases. Fig. 7B shows the hysteresis boundary in the (α, X_f) space. Again the hysteresis boundary is possible only for values of X_f larger than a certain value, i.e. 0.12 g/L. For increasing the values of X_f , the hysteresis domain also increases. The effect of the dilution rate is shown in Fig. 7C. It can be seen that the hysteresis is confined to values of α smaller than 0.052. The hysteresis multiplicity can also occur when the dilution rate is selected as the manipulated variable. Fig. 8 shows an example of hysteresis for the model parameters given in Tab. 1. The output multiplicity occurs for dilution rates in the range of 0.33 h^{-1} to 0.36 h^{-1} . Similar branch sets to Figs. 7A–D can be constructed that delineate the effect of the different operating parameters on the hysteresis. However this effect is chosen to be shown directly on the continuity diagrams. Fig. 9A demonstrates the effect of pH_1 . It is evident that as the pH_1 values decrease, the hysteresis behavior is attenuated. When the value of pH_1 is reduced to 6.0, a stable behavior is found for all values of the dilution rates. Similarly, Fig. 9B shows that a decrease in the values of pH_2 also stabilizes the behavior of the bioreactor. Fig. 10A however shows that an increase in the cell concentration of the feed (X_f) reduces the

multiplicity region. For values of $X_f = 12 \text{ g/L}$, the hysteresis disappears. Finally, Fig. 10B shows that an increase in α also attenuates the hysteresis multiplicity.

3.1 Case of No Additional Seed Tank

The analysis carried out in the previous sections has demonstrated that the case when the bioreactor is not equipped with an additional seed tank ($\alpha = 0$) is an important case that

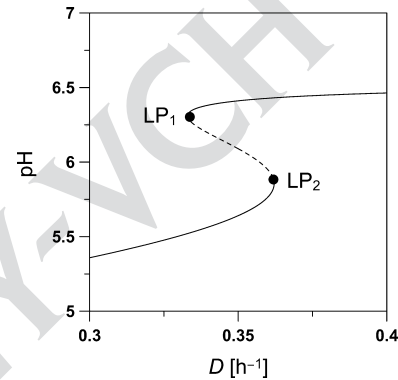


Figure 8. Continuity diagrams showing the hysteresis in the dilution rate D . (Solid line, stable branch; dash line, unstable branch; LP_1 and LP_2 are static limit points).

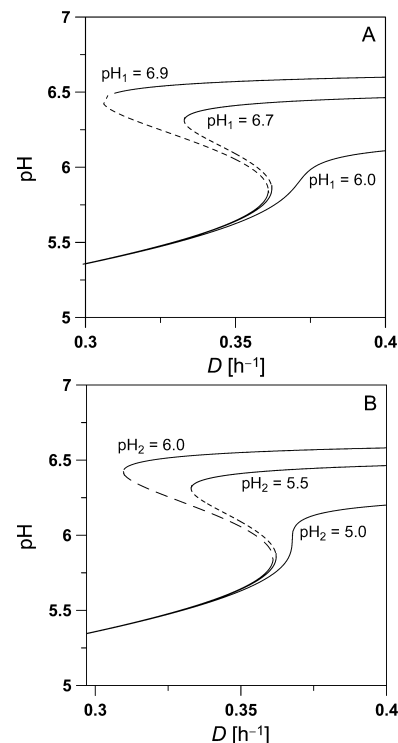


Figure 9. Continuity diagrams showing the effect on the hysteresis of Fig. 8: (A) changes in pH_1 . (B) changes in the pH . (Solid line, stable branch; dashed line, unstable branch).

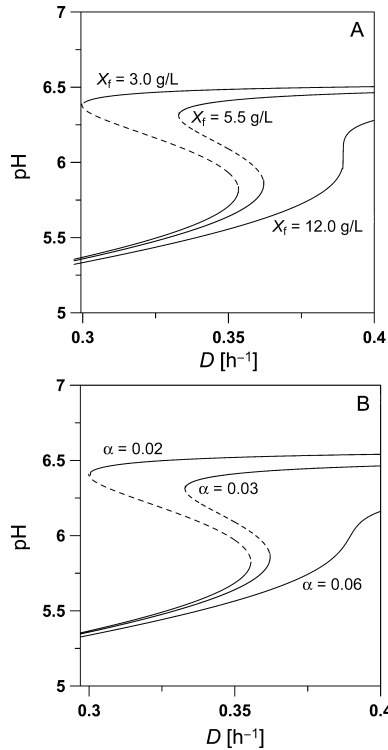


Figure 10. Continuity diagrams showing the effect on the hysteresis of Fig. 8: (A) changes in X_f , (B) changes in α . (Solid line, stable branch; dashed line, unstable branch).

should be treated separately. For this case, the model steady state equations (Eqs. (10–13)) become:

$$-DX + \mu([H^+])X = 0 \quad (39)$$

$$D(S_f - S) - \sigma([H^+])X = 0 \quad (40)$$

$$-DP + \pi([H^+])X = 0 \quad (41)$$

$$D([H^+]_1 - [H^+]) + v([H^+])X = 0 \quad (42)$$

The primary difference in terms of steady state behavior is that the model predicts (for the case of $a = 0$) the existence of a total washout, ($X = 0$, $S = S_f$, $P = 0$, $[H^+] = [H^+]_1$), as a trivial steady state solution. The additional non-trivial steady state occurs when

$$F := \mu([H^+]) - D = 0 \quad (43)$$

Substituting for the expression of $\mu([H^+])$ yields the following quadratic equation

$$\frac{D}{K_2}[H^+]^2 + [H^+](D - \mu_0) + DK_1 = 0 \quad (44)$$

This equation provides steady state values of $[H^+]$ as a function of D , while the rest of species concentrations are given by

$$X = -\frac{D([H^+]_1 - [H^+])}{v([H^+])} \quad (45)$$

$$S = S_f - \frac{\sigma([H^+])X}{D} \quad (46)$$

$$P = \frac{\pi([H^+])X}{D} \quad (47)$$

The only operating parameters of the model that can produce multiplicities are $[H^+]_1$ and D . However it is straightforward to check that the model cannot predict any multiplicity as $[H^+]_1$ is varied. When, on the other hand, the dilution rate is selected as the manipulated variable, Eq. (43) predicts a simple saddle-node bifurcation, defined by $F = 0$, $F_{[H^+]} = 0$ and $F_{[H^+][H^+]} \neq 0$. The condition $F_{[H^+]} = 0$ requires, from Eq. (43), that $m^*([H^+]) = 0$. This occurs at the limit point (LP) defined by

$$[H^+] = \sqrt{K_1 K_2}, \quad D_{LP} = \frac{\mu_0 \sqrt{K_2}}{2\sqrt{K_1} + \sqrt{K_2}} \quad (48)$$

The wash-out line crosses with the non-trivial steady state at a bifurcation point (BR) defined by substituting $[H^+] = [H^+]_1$ in Eq. (43) to yield

$$D_{BR} = \frac{\mu_0 [H^+]_1}{K_1 + [H^+]_1 + [H^+]_1^2 / K_2} \quad (49)$$

Depending on the position of the limit point (LP) (Eq. (48)) and the bifurcation point (BR) (Eq. (49)), different behavior in the model can be obtained. Therefore the condition $D_{BR} = D_{LP}$ represents a boundary for the model. This condition is equivalent simply to

$$[H^+]_1 = \sqrt{K_1 K_2} \quad (50)$$

For this condition, the bifurcation diagram (see Fig. 11A) presents a perfect pitchfork. Both the limit point (LP) and the bifurcation point BR collapse in one point. However, as the meaningful existence of cells (i.e. $X > 0$) (requires, from Eq. 45, $[H^+] > [H^+]_1$), the unstable upper branch is physically unrealistic. For dilution rates smaller than D_{LP} the operation of the bioreactor leads to the non-trivial lower steady state while for dilution rates larger than D_{LP} , total washout occurs. The case of $[H^+]_1 < \sqrt{K_1 K_2}$ is shown in Fig. 11B. In this case, the bifurcation point BR is smaller than the limit point. The upper unstable branch is still physically unrealistic. Between BR and LP points, there is multiplicity in the form of bistability between the lower non-trivial steady state and the total washout. Different initial conditions can lead to either branch. The case of $[H^+]_1 > \sqrt{K_1 K_2}$ is shown in Fig. 11C. It can be seen that the position of points BR and LP has changed. However since the whole upper branch is physically unrealistic then this case is similar to the case of perfect pitchfork (see Fig. 11A).

A final case to be treated, and that has arisen in the analysis of the general model, is when the seed tank is cell-free, (i.e. $a \neq 0$. and $X_f = 0$). This situation corresponds to the case when

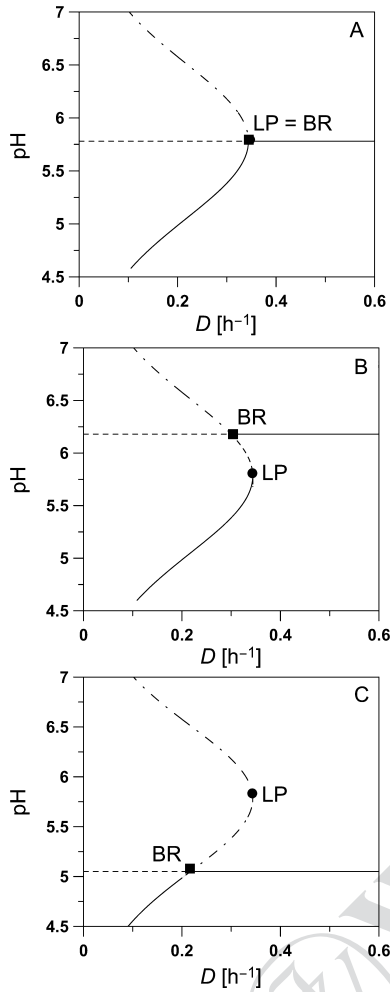


Figure 11. Continuity diagrams for the case of $a = 0$. (A) $[H^+]_1 = \sqrt{K_1K_2}$, (B) $[H^+]_1 < \sqrt{K_1K_2}$, (C) $[H^+]_1 > \sqrt{K_1K_2}$. (Solid line, stable branch; dashed line, unstable branch; semi-dash line, unstable and physically unrealistic branch; BR, bifurcation point, LP limit point).

the additional seed tank consists only of product P_f and hydrogen ion $[H^+]_2$ feeds. The original model equations (Eqs. (11–13)) are unchanged with the exception of Eq. 10 that becomes,

$$-DX + \mu X = 0 \tag{51}$$

For this case, the model always admits as a steady state solution the following “modified” washout solution

$$X = 0, S = \frac{S_f}{1+a}, P = \frac{aP_f}{1+a}, [H^+] = \frac{[H^+]_1}{1+a} + \frac{a[H^+]_2}{1+a} \tag{52}$$

The non-trivial steady state solution corresponds to

$$\mu = D \tag{53}$$

and

$$X = -\frac{D\left(\frac{[H^+]_1}{1+a} + \frac{a[H^+]_2}{1+a} - [H^+]\right)}{v([H^+])} \tag{54}$$

The expressions for S and P are identical to Eqs. (16–17). Since the equation defining the pH (Eq. (53)) is the same as the previous example ($a = 0, X_f \neq 0$), therefore when D is selected as the manipulated variable, the same previously discussed pitchfork behavior of Figs. 11A–C occurs. The only difference is that the pitchfork boundary is defined by

$$\frac{[H^+]_1}{1+a} + \frac{a[H^+]_2}{1+a} = \sqrt{K_1K_2} \tag{55}$$

This equation is naturally reduced to (Eq. (50)) when $a = 0$.

4 Conclusions

In this paper, the effect of design and operating parameters on the steady state behavior of a bioreactor for cheese pre-fermentation were analyzed. The singularity theory was used to classify the different multiplicities the model can predict. For the case when the bioreactor is equipped with a seed tank, the analysis has shown that input and output multiplicities can only appear in the model when either the dilution rate or the ratio of seed to substrate feed rates is selected as the manipulated variable. The rest of the operating parameters cannot induce such multiplicities. In this regard, a pitchfork singularity can only occur with variations in the ratio of feeds while hysteresis is possible with variations of any of the two parameters. When pitchfork singularity occurs, the improvement of the stability of the bioreactor can be achieved by a reduction in the dilution rate, an increase in the feed pH, a decrease in seed tank pH or an increase in the concentration of the cells in the feed. When hysteresis occurs, as the ratio of feeds is manipulated, the instability of the bioreactor can be reduced by a decrease in the feed pH or a decrease in the feed concentration. When, on the other hand, hysteresis occurs for variations in the dilution rate, then the stability can be improved through reducing the pH of the feed, increasing the ratio of feed rates or increasing the feed concentration. The paper also analyzed the case when the bioreactor is operated without any seed tank. In this case it was shown that when the dilution rate is chosen as the manipulated variable, the behavior of the bioreactor is reduced to a pitchfork. A simple algebraic equation was derived between the feed pH and the kinetic parameters associated with the growth rate of the cells. The algebraic equation can be used to select the values for the feed pH that reduces the multiplicity in the bioreactor.

A final note should be made about the usefulness of these results. While the theoretical tools used in this analysis may seem somehow sophisticated, they are well documented in the literature and they can be readily applied to other kinetic models for cheese pre-fermentation as well to other fermentation processes. The usefulness of these tools is that they lead most often to analytical equations that describe the operation of the bioreactor. Should the kinetic model be accurate (experimentally validated), then these analytical equations can provide real insight into the operation of the industrial bioreactor. It allows an early detection of difficult operating regions in bioreactors. This would allow the removal or at least the reduction of these operational problems in the early stage of process design, and this would ultimately improve the operability of the bioreactor.

Symbols used

D	dilution rate [h^{-1}]
F_1	lactose feed rate to bioreactor [L/h]
F_2	lactose feed rate to bioreactor from the seed tank [L/h]
F_3	exit feed rate from the bioreactor [L/h]
K_1	kinetic constant for the respective specific growth rate [g/L]
K_2	kinetic constant for the respective specific growth rate [g/L]
K_3	kinetic constant for respective specific substrate consumption rate [g/L]
K_4	kinetic constant for respective specific substrate consumption rate [g/L]
K_5	kinetic constant for respective specific production rate [g/L]
K_6	kinetic constant for respective specific production rate [g/L]
P	lactic acid concentration [g/L]
P_f	lactic acid feed concentration [g/L]
S	lactose concentration [g/L]
S_f	lactose feed concentration [g/L]
V	volume of the bioreactor [g/L]
X	cell concentration [g/L]
X_f	cell concentration of the feed [g/L]
α	ratio of the seed to the substrate feed rates
μ	specific growth rate [h^{-1}]
μ	maximum specific growth rate [h^{-1}]
π	specific production rate [h^{-1}]
π_0	maximum specific production rate [h^{-1}]
σ	lactose consumption rate [h^{-1}]
σ	maximum lactose consumption rate [h^{-1}]
ν	hydrogen ion production rate [h^{-1}]
ν	maximum hydrogen ion production rate [h^{-1}]

References

- [1] R. Aguilar, J. Gonzalez, M. A. Barron, R. Martinez-Guerrea, R. Maya-Yescas, Robust PI^2 controller for continuous bioreactors, *Process Biochem.* **2000**, *36*, 1007–1013.
- [2] R. G. Dondo, D. Marques, Optimal control of a batch bioreactor: a study on the use of an imperfect model, *Process Biochem.* **2001**, *37*, 379–385.
- [3] T. K. Radhakrishnan, S. Sundaram, M. Chidambaram, Non-linear control of continuous bioreactors, *Bioprocess Eng.* **1999**, *20*, 173–178.
- [4] R. Ramaswamy, T. K. Cutright, H. K. Qammar, Control of a continuous bioreactor using model predictive control, *Process Biochem.* **2005**, *40*, 2763–2770.
- [5] R. Sousa Jr, G. P. Lopes, G. A. Pinto, P. I. F. Almeida, R. C. Giordano, GMC-fuzzy control of pH during enzymatic hydrolysis of cheese whey proteins, *Comp. Chem. Eng.* **2004**, *28*, 1661–1672.
- [6] S. S. E. H. Elnashaie, P. Garhyan, *Conservation Equations and Modeling of Chemical and Biochemical Processes*, Marcel Dekker **2003**.
- [7] L. P. Russo, B. W. Bequette, Impact of process design on the multiplicity behavior of a jacketed exothermic CSTR, *AIChE J.* **1995**, *41*, 135–147.
- [8] L. P. Russo, B. W. Bequette, Effect of process design on the open-loop behavior of a jacketed exothermic CSTR, *Comp. Chem. Eng.* **1996**, *20*, 417–426.
- [9] L. P. Russo, B. W. Bequette, Process design for operability: a styrene polymerization application, *Comp. Chem. Eng.* **1997**, *21*, 571–576.
- [10] A. E. Gamboa-Torres, A. Flores-Tlacuahuac, Effect of process modeling on the nonlinear behaviour of a CSTR reactions. $A \rightarrow B \rightarrow C$, *Chem. Eng. J.* **2000**, *77*, 153–164.
- [11] P. Garhyan, S. S. E. H. Elnashaie, Bifurcation analysis of two continuous membrane fermentor configurations for producing ethanol, *Chem. Eng. Sci.* **2004**, *59*, 3235–3268.
- [12] S. S. E. H. Elnashaie, N. F. Mohamed, Implications of bifurcation/chaos on the design, operation and control of industrial riser-reactor FCC units, *Chem. Eng. Commun.* **2004**, *191*, 813–831.
- [13] M. H. Jorgensen, K. Nikolajsen, Mathematic model for lactic acid formation with *Streptococcus cremoris* from glucose, *Appl. Microbiol. Biotech.* **1987**, *25*, 313–316.
- [14] [14] A. De Raucourt, D. Girard, Y. Prigent, P. Boyaval, Lactose continuous fermentation with cells recycled by ultrafiltration and lactate separation by electrodialysis: modelling and simulation, *Appl. Microbiol. Biotechnol.* **1989**, *30*, 521–527.
- [15] H. Ohara, K. Hiyama, T. Yoshida, Kinetics of growth and lactic acid production in continuous and batch culture, *Appl. Microbiol. Biotechnol.* **1992**, *37*, 544–548.
- [16] P. L. Yeh, R. K. Bajpai, E. L. Iannotti, An improved kinetic model for lactic acid fermentation, *J. Ferm. Bioeng.* **1991**, *71*, 75–77.
- [17] H. Ohara, K. Hiyama, T. Yoshida, Non-competitive product inhibition in lactic acid fermentation from glucose, *Appl. Microbiol. Biotechnol.* **1992**, *36*, 773–776.
- [18] H. Funahashi, J. H. Lee, S. Ensari, H. C. Lim, Experimental studies of cheese prefermentation; a mathematical model reflecting the pH effect, *Milchwissenschaft* **2000**, *55*, 75–78.
- [19] J. H. Lee, H. C. Lim, Multiplicity and stability analysis of continuous pre-fermentation of cheese culture, *Process Biochem.* **1999**, *34*, 467–475.
- [20] V. Balakotaiah, D. Luss, Structure of the steady state solutions of lumped parameter chemically reacting system, *Chem. Eng. Sci.* **1982**, *37*, 1611–1615.
- [21] A. Ajbar, On the existence of oscillatory behavior in unstructured models of bioreactors, *Chem. Eng. Sci.* **2001**, *56*, 1991–1997.
- [22] A. Ajbar, Classification of stability behavior of bioreactors with wall attachment and substrate inhibited kinetics, *Biotechnol. Bioeng.* **2001**, *72*, 166–176.
- [23] A. Ajbar, Classification of static and dynamic behavior in chemostat for plasmid-bearing, plasmid-free mixed recombinant cultures, *Chem. Eng. Commun.* **2002**, *189*, 1130–1154.
- [24] M. Golubitsky, D. Schaeffer, *Singularities and Groups in Bifurcation Theory*, Vol. 1, Springer, Berlin, New York **1985**.
- [25] E. J. Doedel, *Auto: Software for Continuation and Bifurcation Problems in Ordinary Differential Equations*, California Institute of Technology, Pasadena, California **1985**.

DOI: 10.1002/elsc.200720215

Research Article: Cheese pre-fermentation is a process that is strongly dependent on hydrogen ions since it is known that the pH of milk changes with cell growth and lactic acid production. A fermentation model that includes the effect of the pH on the growth kinetics was previously developed for *Lactococcus*. The analysis of this model carried out in this paper shows how the design and the operating parameters can influence the stability of the bioreactor and consequently help improve the operability of the unit.

Study of the Operability of a Continuous Bioreactor for the Pre-fermentation of Cheese Culture

A. Al-Rabiah and A. Ajbar*

Eng. Life Sci. 2007, 7 (6),

